PROCEEDINGS, Thirty-Seventh Workshop on Geothermal Reservoir Engineering
Stanford University, Stanford, California, January 30 - February 1, 2012
SGP-TR-194

# MODELING COUPLED THERMAL-HYDROLOGICAL-MECHANICAL PROCESSES DURING SHEAR STIMULATION OF AN EGS WELL

Sharad Kelkar[1], Kayla Lewis[2], Steve Hickman[3], Nicholas C. Davatzes[4], Daniel Moos[5], and George Zyvoloski[2]

[1] Los Alamos National Laboratory, Los Alamos, New Mexico, 87545, USA. kelkar@lanl.gov
[2] Los Alamos National Laboratory, Los Alamos, New Mexico, 87545, USA.
[3] USGS, Menlo Park, CA, USA.
[4] Temple University, Philadelphia, PA, USA.
[5] Baker Hughes, Palo Alto, CA, USA

## ABSTRACT

We are developing a general purpose computational code, FEHM that models coupled thermal-hydrological-mechanical (THM) processes during multi-phase fluid flow and deformation in fractured porous media. The code is control volume -finite element based. The equations representing all three of the THM processes being considered are formulated simultaneously. Nonlinearities in the equations and the material properties are handled using a full Jacobian Newton-Raphson technique. The code incorporates several models of stress dependent permeability. We present 3-dimensional models of the evolution of permeability enhancement during shear stimulation using published data from the Desert Peak Geothermal Field in Nevada, including sensitivity studies for parameters and boundary conditions that also span the ranges published for the Brady's field in Nevada, USA.

## INTRODUCTION

Hydraulic stimulation is a technique often used to improve the formation permeability near a wellbore and to connect to the natural productive zones in a reservoir. In Enhanced Geothermal Systems (EGS), stimulation can enhance permeability by inducing new tensile fractures or through dilatant shearing of natural fractures. Even under the conditions when tensile failure (hydrofracturing) dominates, shear failure can play an important role as evidenced by induced microseismicity. This impact is most pronounced away from the wellbore and in fluid leak off from a hydrofracture in formations with low matrix permeability.

There are some important parallels as well as differences between stimulation of EGS versus petroleum reservoirs. In oil, gas shale or tight gas reservoir, production requires highly permeable pathways connecting the formation to the well so as to rapidly drain the stimulated volume. On the other hand, EGS requires long-term contact between the fluid and the matrix through a distributed network of fractures to extract heat efficiently. In EGS systems, hydraulic conductivity needs to be sufficiently high to inject and produce heat-transfer fluids at practical rates; however, creating a highly localized zone of high conductivity is not desirable as this can lead to thermal drawdown and short-circuiting. For these reasons, it is not desirable to subject an EGS well to a massive hydrologic fracturing treatment similar to those practiced in traditional petroleum reservoirs.

EGS systems can be of many types. The original Hot Dry Rock concept (Kelkar et al. 2011a) involved a pair of wells drilled in a tight crystalline formation that lacked the ability to naturally produce geothermal fluids. The concept being currently pursued by many projects is that of an existing hydrothermal reservoir with an outlier well that lacks sufficient connectivity with the productive portions of the reservoir (DOE 2009). A EGS project that falls in this later class is under way at the Desert Peak geothermal field in Nevada (Zemach et al. 2009; Chabora et al. 2012) – and the modeling efforts discussed in the present paper are pertinent to such EGS systems.

The hydraulic fracturing treatments utilized in the petroleum industry involve the injection of viscous fluids at sufficiently high pressures to overcome the minimum in-situ principal stress and the rock strength in the formation, creating tensile fractures that may propagate over hundreds of meters. Such hydraulic fractures, often with the use of proppants, create high conductivity pathways that can rapidly drain formation fluids to the wellbore. In contrast, the hydraulic stimulations being considered in EGS applications involve water injection at pressures below the minimum in situ stress, but above the threshold required for shear fracturing. Barton et al. (1988) discuss the concept of critically stressed

fractures in the earth's crust. The state of stress in geothermal systems can often be such that at moderate wellhead pressures optimally oriented natural fractures can reach the critical state, resulting in shear stimulation. Moos et al. (2011) discuss an integrated study involving tensile as well as shear stimulation.

Results of stimulation treatments are controlled by hydrologic and mechanical properties of the formation (including natural fractures), in-situ stresses, properties of the injected fluid and treatment parameters including flow rate, pressure, and temperature. Shear stimulation treatments, in which borehole fluid pressure remains below the minimum principal stress magnitude can last weeks to months; thus thermo-mechanical as well as poro-mechanical effects become important. The ability to model the coupled THM processes in fractured geological formations at high temperature is important in analyzing EGS stimulation treatments.

## CODE DESCRIPTION

The reservoir simulation problems of interest to EGS systems range from behavior in the near-wellbore region to the reservoir, thus spanning length-scales from tens of centimeters to kilometers, and temporal scales of hours to years. At these scales, large variations in fluid pressure, temperature and stresses are expected. These reservoirs are fracture dominated and inhomogeneous with large variations in material properties. In addition, material properties such as permeability and Young's modulus can vary by several orders of magnitude and are highly nonlinear functions of the state variables pressure (P), temperature (T), and stress ($\sigma_{ij}$).

Our approach has been to build an integrated code capable of solving fully coupled nonlinear continuum equations of mass balance, heat transfer, and mechanical deformations in fractured porous media. We use Newton-Raphson outer iterations with a complete Jacobian and efficient linear equation solvers. We have built on the code FEHM (Zyvoloski 2007), originally developed to model non-isothermal fluid flow in Hot Dry Rock geothermal reservoirs. FEHM has been developed extensively under projects on conventional/unconventional energy extraction (geothermal, oil, and gas), radionuclide and contaminant transport, watershed management, and $CO_2$ sequestration. It is a continuum code based on the control volume finite element approach, capable of handling non-isothermal, multiphase, multi-component fluid flow, heat transfer and chemical transport in dual porosity, dual permeability media on unstructured grids. FEHM uses an efficient approach for evaluating thermodynamic functions using lookup tables and polynomial approximations to calculate derivatives in the computations. FEHM also uses a novel technique of uncoupling the material coefficients from the geometric integrals involving shape functions. This allows us to pre-compute the geometric integrals at the beginning of the simulation, saving significant computational resources during iterative solutions of nonlinear problems.

We have incorporated static mechanical force balance equations in FEHM using the finite element approach. The materials can display linear or nonlinear, elastic or elastic-plastic behavior, including anisotropic properties. Spatially varying material properties are mapped from nodes onto finite elements using shape function interpolations. Coupling between the fluid flow, heat transfer and mechanical force balance equations occurs both through the explicit occurrence of terms in balance equations such as the effective stress and thermal stress, as well as through the dependence of various coefficients on the state variables. The goal of our work is to develop a code capable of handling explicit as well as implicit coupling.

The state variables computed by the code at each node are P, T, and displacement components $u_x$, $u_y$, and $u_z$. We cast the mass and energy balance equations in terms of the control volumes associated with each node. The mechanical force balance equations, on the other hand, are cast over the first order finite elements defined by the connected nodes. However, material failure and plastic yield criteria such as Mohr-Coulomb, Von Mises or Drucker-Prager (e.g. Jaeger and Cook, 1979) use stress as the state variable rather than the displacements. We use the finite element approach to evaluate stresses at the first order Gauss point from the displacements, as this is known to be of higher order accuracy than calculating average stresses at the nodes (Bathe, 1982). The fluid mass balance equations are solved using the control volume approach. Every node has a set of nodes connected to it. Every pair of connected nodes forms an edge. A control volume is associated with each node, defined by interfaces at midpoints of edges connected to that node. This approach requires permeabilities to be assigned at interfaces between connected pairs of nodes. These are commonly computed from the nodal values using harmonic averaging; an approach known to conserve mass. We treat these interfacial permeabilities, rather than the nodal values, as the stress-dependent quantities. The nodes and the edges together also define first order hexagonal finite elements over the domain. Since there may be several elements that share the edge defined by a pair of nodes, the stress value for each

element is used to compute the contribution to the flow from the respective element. Many functionalities of the code have been verified against commercially available codes (Kelkar et al., 2011b; Class et al., 2009).

In fault dominated reservoirs permeability is perhaps the parameter most sensitive to variations in P, T, and $\sigma_{ij}$ (and displacements). For example, Evans et al. (2005) noted a 15-fold increase in the injectivity upon hydraulic stimulation at the Soultz EGS reservoir in France. Sensitivity of fracture permeability to aperture changes resulting from shearing or changes in normal stress is well recognized (e.g. Barton et al. 1985; Gangi 1978; Bai et al., 1999; Elsworth and Xiang, 1989). Laboratory tests have shown as much as a two order of magnitude increase in fracture permeability upon shear displacement (e.g. Lee and Cho, 2002). In FEHM we have incorporated several models as user defined options for simulating the role of stress/deformation on changes in the permeability tensor.

**Permeability-Stress Model Set-up**

In this study, a model of permeability change due to shear failure was used. The condition for shear failure is derived from the Mohr-Coulomb criterion, which is conveniently described by defining a quantity we will call 'excess shear stress' by

$$\tau_{excess} = |\tau| - S_o + \mu * \sigma^{eff}$$

…… Eq. 1

where $|\tau|$ is the absolute value of the shear stress on a plane, $\sigma^{eff}$ is the effective normal stress (i.e. normal stress minus the pore pressure) acting on that plane, $S_o$ is cohesion, and $\mu$ is the coefficient of sliding friction on the plane. If $|\tau_{excess}| > 0$ then shear failure will occur.

$\sigma^{eff}{}_1, \sigma^{eff}{}_2, \sigma^{eff}{}_3$ are defined as the maximum, intermediate, and minimum effective principal stresses respectively. The maximum value of the 'excess shear' stress $\tau_{excess}$ is given by (Jaeger and Cook 1979):

$$\tau_{excess}(\max) = \frac{1}{2}(\sigma^{eff}{}_1 - \sigma^{eff}{}_3)(\mu^2 + 1)^{1/2} - \frac{1}{2}\mu(\sigma^{eff}{}_1 + \sigma^{eff}{}_3)$$

…… Eq. 2

and occurs on a plane that is orientated at an angle $\beta$ with respect to the maximum principal stress ($\sigma_1$) given by

$$\tan(2\beta) = -\frac{1}{\mu}$$

…….Eq. 3

For the purpose of this work we model a formation with ubiquitous preexisting fractures so that a fracture with optimal orientation is always available for shear failure. However, the FEHM model is capable of handling user-specified fracture orientations.

Upon failure, the modified permeability is obtained by multiplying the initial permeability (as well as Young's modulus) by user specified factors that can have three different values along the principal directions of the permeability tensor. The principal axis of the permeability tensor are assumed to align with the frame of reference rotated so that x' and y' axis lie in the fracture plane. The modified principal permeabilities are calculated by multiplying the original permeabilities by user specified factors. The modified permeability tensor is then rotated back to the original grid coordinate frame. In the current version of the code, the off-diagonal terms in the permeability tensor in the grid coordinate system are neglected; i.e. the component of the pressure gradient along a particular coordinate direction can give rise to flow only in that direction.

Although not used in the model under current discussion, the code is capable of simulating material softening by reducing the Young's modulus in each direction by a user specified factor. Work is also under way for coupling plastic material deformation with permeability models.

**NUMERICAL MODEL SETUP**

The example presented here used a model domain of 2 km by 2 km in the horizontal directions and 1 km in the vertical direction (Figure 1). The Z axis was aligned with the maximum principal stress, which was taken to be vertical. The X axis was taken to be horizontal and aligned with the least principal stress. There were a total of 79,365 computational nodes. Injection was at a point at the center of the X and Z dimensions, and ¼ of the way from the boundary along the Y axis. The grid spacing was decreased near the injection point to improve model resolution.

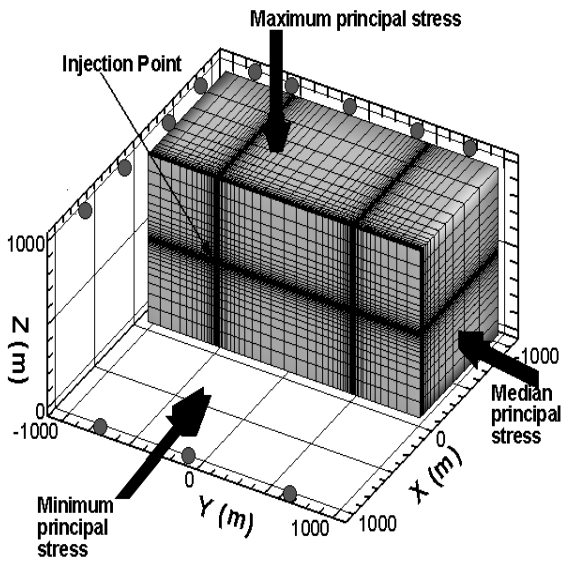


Figure 1. A cut-away view of the computational grid, also showing the principal stress directions.

The example discussed here assumes isotropic values for the permeability multiplies for the sake of simplicity, although the FEHM model is capable of handling more general cases. On a physical basis (confirmed by laboratory tests, e.g. Auradou et al., 2006), it can be expected that upon shear stimulation the permeabilities within the plane of shearing will be enhanced, while that normal to the plane of shearing may not experience as much change. The case of anisotropic multipliers will be studied in future work.

The FEHM model is capable of handling gravity; however, for the sake of simplicity, the examples presented here did not include gravity. This will be addressed in future work. Fluid flow boundary conditions were chosen to be such that pressure was held at the constant initial value on the exterior faces of the model volume, and a constant specified pressure of 13.1 MPa was applied at the injection point. The heat flow boundary conditions were taken to be no flow of heat at the external boundaries of the model volume and a constant temperature was specified for the injected fluid.

The parameter values used in the example are summarized in Table 1. These values were selected from Lutz et al. (2009, and2010) and Hickman and Davatzes (2010) as being in the range of values most suitable for the stimulation interval in the Desert Peak well 27-15 (3000 to 3500 ft depth). Note that the injection pressure (13.1 MPa) was selected to be just below the magnitude of the least principal stress (13.8 MPa), so as to favor shear stimulation without initiating hydraulic fracturing. The injection temperature was selected to approximately represent fluid injection temperatures used during the shear stimulation phase in Desert Peak well 27-15. Site specific heat capacity and thermal conductivity values were not available, thus generic values were used. The permeability multiplier (i.e., the increase in permeability realized upon shearing) was selected as 15, to fall somewhat below the enhancement in fracture permeability upon shearing measured by Lee and Cho (2002).

Table 1. Parameter values used in the present model.

| PARAMETER | VALUE |
|---|---|
| Formation temperature | $190^0$ C |
| Initial pore pressure | 9 MPa |
| Bottom hole injection pressure | 13.1 MPa |
| Injection temperature | $170^0$ C |
| Principal in situ stresses | |
| Maximum | 22.6 MPa (vertical) |
| Intermediate | 18.1 MPa |
| Minimum | 13.8 MPa |
| Thermal conductivity | 3 W/m/K |
| Heat capacity | 820 J/kg/K |
| Porosity | 10% |
| Initial permeability*thickness | 9 md.m |
| Shear failure-permeability model parameters | |
| Friction Coefficient | 0.8 |
| Cohesion | 2 MPa |
| Permeability multiplier (all directions) | 15 |
| Young's modulus | 30 GPa |
| Poisson' ratio | 0.15 |
| Coeffficient of Thermal Expansion | $10^{-4}$ /$^0$C |
| Biot poroelastic parameter | 0.5 |

## RESULTS AND DISCUSSION

### Characteristics of Model Behavior

Figure 2 shows the modeled normalized injection rate versus time obtained for the model discussed above. The injection-time history is normalized against convenient values to emphasize different injection rate behaviors (Stages I, II, and III) associated with contributions of distinct processes that dominate at different times during the simulated stimulation.

At early times, shown as Stage I in Figure 2, the response is most similar to a system with fixed permeability and fluid properties. Sensitivity analysis reveals that injection rate constant pressure in this

stage is most sensitive to initial permeability and fluid viscosity.

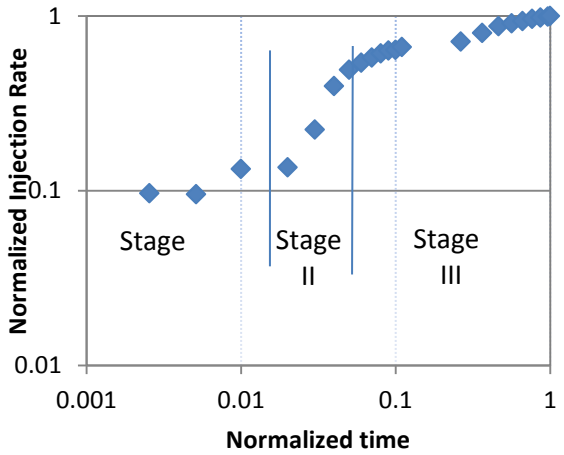


Figure 2. Simulated normalized injection rate versus time.

In Stage II, the injection rate at constant pressure begins to climb in response to the stress-dependence of permeability. This transition results from a combination of Mohr-Coulomb failure and injection-induced cooling of the formation at ever-increasing distances from the wellbore, with the latter resulting in thermal contraction. The superposition of thermal stresses in the formation on the ambient stress state promotes shear failure above that which would be expected due to increased fluid pressures alone. This produces a positive feedback where higher rates of flow allow for the cooler fluid to penetrate deeper into the formation, leading to a continuing increase in permeability. In addition to injection pressure and temperature, the onset of this Stage is most sensitive to material properties such as cohesion, coefficient of friction, Young's modulus and coefficient of thermal expansion. Other properties such as conductivity and heat capacity, have an important, but lesser impact.
In Stage III, the flow rate continues to increase at a rate lower than that in Stage II. The rate of increase is lower because the region nearest to the injection point has already gone through permeability enhancement, and the fluid traveling further out gets warmer and the pressure drops off. The transition from Stage II to III is sensitive to the permeability multiplier used in the stress-permeability model.

Sensitivity studies comparing a line source with a point source showed that the relative onset and magnitude of the three regions in Figure 2 is also sensitive to the geometry of the injection interval.

## Heuristic Investigation of Hydro-Shear in Desert Peak Well 27-15

Figure 3 shows a comparison between the injection rate calculated by the model and the data reported by Chabora et al. (2012) for the EGS stimulation of Desert Peak well 27-15 during the shear stimulation phase; from September 13 to 25, 2010; at wellhead injection pressures of 3.1 MPa (450 psi) and initial flow rates around 7 gpm. A very short term test prior to stimulation in this interval yielded a permeability-thickness product of 9 md-m. In this model example we had to adjust the product to 2.8 md-m (over an injection interval of 4.7 m) to get a reasonable match – not an unreasonable adjustment given the simplicity of the model and the short duration of the field test. It is noteworthy that despite the simplicity of the model, the two curves exhibit the same range of flow rates. The model predicts the onset of significant shear stimulation due to excess fluid pressure and thermal stresses much sooner than that actually observed during the EGS stimulation. Our future work will evaluate the parameter ranges needed to obtain a better fit between model and observations, thus solving for key formation and borehole properties.

Although not shown here, using a source distributed over a much longer interval of the bore hole (150 m) we obtained model flow rates much lower than the flow rate data if the initial permeability-thickness was kept the same order of magnitude as the measured value of 9 md-m. It is not unreasonable to expect that injected fluids will exit the wellbore at a few discrete zones, as implied by temperature perturbations noted both prior to stimulation (Davatzes and Hickman, 2009) and post stimulation (Hickman et al., 2011). This behavior will be studied in future work.

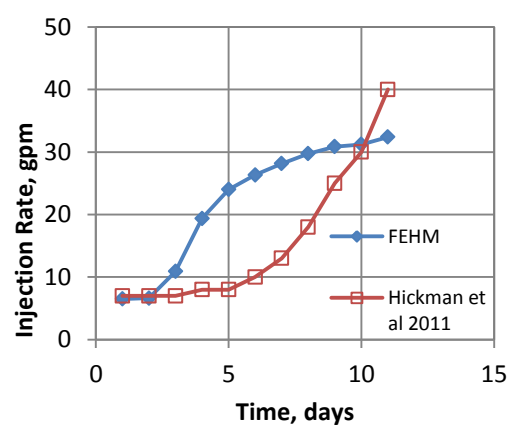


Figure 3. Comparison of model results using a localized source with field data from the EGS stimulation in Desert Peak well 27-15 (Chabora et al. (2012). This model used the parameters listed in Table 1.

Model simulations show that in the long-term hydro-shear stimulations akin to those induced in DP 27-15, the evolution of flow rate during the injection

timeline is highly sensitive to thermal expansion coefficient (alpha) and injection temperature (Figure 4). Lower values of thermal expansion coefficient induce much smaller thermal stresses. Based on results not shown here, we judge that this effect is somewhat compensated by reducing injection temperature, however, the increase in permeability is still less than that in the first case. As a result, injection rates are lower for the second case. In addition, the onset of the stimulation also occurs at a later time for the lower value of alpha.

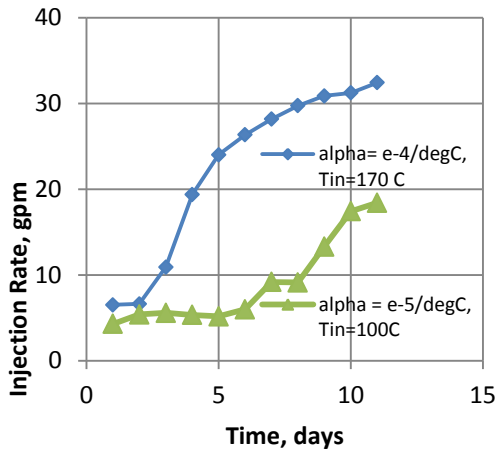


Figure 4. Sensitivity of flow rate to thermal expansion coefficient and injection temperature. The upper (blue) curve used the same model parameters as used previously (Figure 3 and Table 1), whereas the lower (green) curve used the lower thermal expansion coefficient and injection temperature shown.

As noted earlier, both the initial formation permeability and the permeability multiplier resulting from shear failure are critical to the temporal evolution of flow rate. To explore this effect, a case is presented where the effect of the reduced coefficient of thermal expansion (Figure 4) is compensated by increasing the permeability multiplier to 100, in addition to dropping the injection temperature to $100^0$C (Figure 5).

It is interesting to note that for this case, the onset of shear stimulation occurs much later than the case with higher thermal conductivity. Once the stimulation starts, the rate increases rapidly due to the high value of the permeability multiplier.

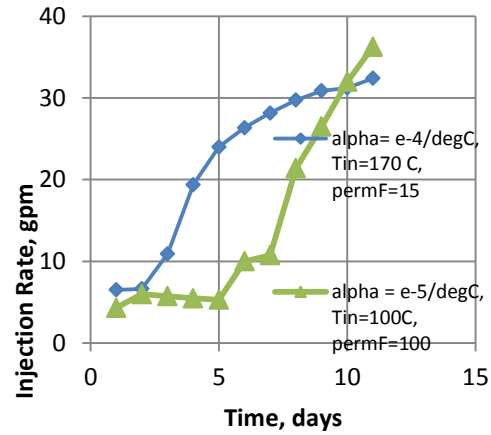


Figure 5. Effect of increasing the permeability multiplier to 100 in addition to reduced alpha and inlet temperature.

## CONCLUSIONS AND FUTURE WORK

We have developed a code capable of modeling coupled THM processes including permeability enhancement due to shear stimulation. Preliminary results of comparing model results against data from the Desert Peak EGS stimulation in well 27-15 are encouraging and reveal three stages of stimulation progression during hydroshear stimulations that involve relatively cool water. These phases are characterized by distinct time-injection rate behavior that is also evident from the hydro-shear stimulation of Desert Peak well 27-15 (Chabora et al., 2012). More extensive sensitivity analysis and history matching with field data are underway to solve for formation characteristics and better diagnose the mechanisms of permeability enhancement, in particular the interplay between effective stress (i.e., fluid pressure) and thermal effects. Tensile stimulation models will be added to simulate the hydraulic fracturing processes, as relevant to the later stages of the Desert Peak EGS stimulation (Chabora et al., 2012). The spatial distributions of pressure, temperature, and stress changes predicted by the model will also be integrated with micro earthquake locations and tracer data, to compare the predicted and observed growth in stimulated volume surrounding the Desert Peak EGS well 25-15.

## ACKNOWLEDGEMENTS

Funding for this work was provided by US DOE Office of Geothermal Technologies under contract No. GT-100036-20685-09. The coupled flow and stress numerical simulations capabilities in FEHM applied for this work were done at LANL under the Zero Emission Research & Technology (ZERT-II) project funded by US DOE through its $CO_2$ sequestration R&D program. Authors would like to

acknowledge valuable discussions with Ezra Zemach of ORMAT and Dr. Saikiran Rapaka of Siemens Corporate Research.

## REFERENCES

Auradou H., Drazer G., Boschan A., Hulin J.P., Koplik J., 2006, "Flow channeling in a single fracture induced by shear displacement. Geothermics 35 (2006) 576-588

Barton N., Bandis S., and Bakhtar K., 1985, "Strength, Deformation and Conductivity Coupling of Rock Joints", Int. J. Rock Mech. Min. Sci. & Geomech. Abstr. Vol. 22, No.3, pp 121-140, 1985.

Barton C.A., Zoback M.D., and Moos D., "Fluid flow along potentially active faults in crystalline rock", Geology, August 1995; v. 23, no. 8. P. 683-686.

Bathe K. J., 1982, "Finite element procedures in engineering analysis", Published by Prentice-Hall Inc., Englewood Cliffs, NJ.

Chabora E., Zemach E., Spielman P., Drakos P., Hickman S., Lutz S., Boyle K., Falconer A., and Robertson-Tait A., 2012, "Hydraulic stimulation of Well 27-15, Desert Peak Geothermal field, Nevada, USA", PROCEEDINGS, Thirty-Seventh Workshop on Geothermal Reservoir Engineering
Stanford University, Stanford, California, January 30 - February 1, 2012

Class, H ; Ebigbo, A ; Helmig, R ; Dahle, HK ; Nordbotten, JM ; et al. "A benchmark study on problems related to CO2 storage in geologic formations", COMPUTATIONAL GEOSCIENCES (DEC 2009) Vol.13, iss.4, spec. iss.SI, p.409-434

DOE 2009, "Geothermal Technologies Program. Multi-Year Research, Development and Demonstration Plan, 2009-2015 with program activities to 2025", U.S. Department of Energy Efficiency Energy, & Renewable Energy Office, http://www.eere.energy.gov/geothermal/plans.html

Elsworth D., and Xiang J., (1989), "A reduced degree of freedom model for thermal permeability enhancement in blocky rock", Geothermics 18, 691-7009

Gangi A.F., 1978, "Variation of whole and fractured porous rock permeability with confining pressure", Int. J. Rock Min. Sci. & Geomech. Abstr. Vol. 15, pp 249-257.

Davatzes N, and Hickman S., 2009, "Fractures, stress and fluid flow prior to stimulation of well 27-15, Desert Peak, Nevada, EGS project", proceedings, 34th workshop on geothermal reservoir engineering, Stanford University, Stanford, California, February 9-11, 2009.

Hickman S., and Davatzes N, 2010, "In-situ stress and fracture characterization for planning of an EGS stimulation in the Desert Peak geothermal field, Nevada", proceedings, 35th workshop on geothermal reservoir engineering, Stanford University, Stanford, California, February 1-3, 2010.

Hickman S., Davatzes N., Zemach E., Stacey R., Drakos P., Lutz S., Rose P., Majer E., and Robertson-Tait A. (2011), "Hydraulic Stimulation of Fracture Permeability in Volcanic and Metasedimentary Rocks at the Desert Peak Geothermal Field, Nevada," presented at the AGU Fall Meeting, Dec 5-9 2011, San Francisco CA.

Jaeger J.E., and Cook N.G.W., 1979, "Fundamental of rock mechanics", 3rd edition, Published by Chapman and Hall Ltd., New York, NY, USA.

Lee H.S., and Cho T.F., 2002, "Hydraulic Characteristics of Rough Fractures in Linear Flow under Normal and Shear Load. Rock Mech", And Rock Eng. (2002) 35 (4), 299-318.

Lutz S.J., Moore J.N., Jones C.G., Suemnicht G.A., and Robertson-Tait A., 2009, "Geological and structural relationships in the Desert Peak geothermal system, Nevada: Implications for EGS development", proceedings, 34th Workshop on Geothermal Reservoir Engineering, Stanford University, Stanford, California, February 9-11, 2009.

Lutz S.J., Hickman S., Davatzes N., Zemach E., drakos p., and robertson-tait a., 2010, "Rock mechanical testing and petrologic analysis in support of well stimulation activities at the Desert Peak geothermal field, Nevada", proceedings, 35th workshop on geothermal reservoir engineering, Stanford University, Stanford, California, February 1-3, 2010.

Kelkar S., WoldeGabriel G., and Rehfeldt K., 2011a, "Hot Dry Rock Geothermal Energy development at Los Alamos National Laboratory: 1970-1995", Final report, LA-14433-HDR, Los Alamos National laboratory, Los Alamos, New Mexico, USA.

Kelkar S., Pawar R., and Hoda N., 2011b, "Numerical Simulation of Coupled Thermal-Hydrological-Mechanical-Chemical Processes

During In Situ Conversion & Production of Oil Shale", proceeding, 31st Oil Shale Symposium, Colorado School of Mines in Golden, Colorado, October 17-19, 2011.

Moos D., Vassilellis G., Cade R., Franquet J., Lacazette A., Bourtembourg E., and Daniel G., 2011, "Predicting shale reservoir response to stimulation in the Upper Devonian of West Virginia", SPE 145849, presented at the SPE Annual Technical Conference and Exhibition, Denver Colorado, USA, 30 October-2 November 2011.

Zemach E., Drakos, P., and Robertson-Tait A. (2009), "Feasibility evaluation of an "in-field" EGS project at Desert Peak, Nevada", *Geothermal Resources Council Transactions*, v. 33, p. 285-295.

Zyvoloski G., 2007, "FEHM: A control volume finite element code for simulating subsurface multi-phase multi-fluid head and mass transfer", Los Alamos National Laboratory Report LA-UR-07-3359, Los Alamos, New Mexico, USA.